

# UCSF

## UC San Francisco Previously Published Works

### Title

Plasma cell deficiency in human subjects with heterozygous mutations in Sec61 translocon alpha 1 subunit (SEC61A1)

### Permalink

<https://escholarship.org/uc/item/8p7654d7>

### Journal

Journal of Allergy and Clinical Immunology, 141(4)

### ISSN

0091-6749

### Authors

Schubert, Desirée  
Klein, Marie-Christine  
Hassdenteufel, Sarah  
[et al.](#)

### Publication Date

2018-04-01

### DOI

10.1016/j.jaci.2017.06.042

Peer reviewed



Published in final edited form as:

*J Allergy Clin Immunol.* 2018 April ; 141(4): 1427–1438. doi:10.1016/j.jaci.2017.06.042.

## Plasma cell deficiency in humans with heterozygous mutations in *SEC61A1*

Desirée Schubert<sup>1,2,3,\*</sup>, Marie-Christine Klein<sup>4</sup>, Sarah Hassdenteufel<sup>4</sup>, Andrés Caballero-Oteyza<sup>1</sup>, Linlin Yang<sup>1</sup>, Michele Proietti<sup>1</sup>, Alla Bulashevskaya<sup>1</sup>, Janine Kemming<sup>1</sup>, Johannes Kühn<sup>1</sup>, Sandra Winzer<sup>1</sup>, Stephan Rusch<sup>1</sup>, Manfred Fliegau<sup>1</sup>, Alejandro A. Schäffer<sup>5</sup>, Stefan Pfeffer<sup>6</sup>, Roger Geiger<sup>7,8</sup>, Adolfo Cavalié<sup>9</sup>, Hongzhi Cao<sup>10</sup>, Fang Yang<sup>10</sup>, Yong Li<sup>11</sup>, Marta Rizzi<sup>12</sup>, Hermann Eibel<sup>1</sup>, Robin Kobbe<sup>13</sup>, Amy L. Marks<sup>14</sup>, Brian P. Peppers<sup>15</sup>, Robert W. Hostoffer<sup>15,16</sup>, Jennifer M. Puck<sup>17</sup>, Richard Zimmermann<sup>3</sup>, and Bodo Grimbacher<sup>1,18,#</sup>

<sup>1</sup>Center for Chronic Immunodeficiency, Medical Center – University of Freiburg, Faculty of Medicine, University of Freiburg, Germany <sup>2</sup>Spemann Graduate School of Biology and Medicine, University of Freiburg, Germany <sup>3</sup>Faculty of Biology, University of Freiburg, Germany <sup>4</sup>Medical Biochemistry & Molecular Biology, Saarland University, Homburg, Germany <sup>5</sup>National Center for Biotechnology Information, National Library of Medicine, National Institutes of Health, Bethesda, Maryland, USA <sup>6</sup>Department of Molecular Structural Biology, Max-Planck Institute of Biochemistry, Martinsried, Germany <sup>7</sup>Institute for Research in Biomedicine, Università della Svizzera italiana, Bellinzona, Switzerland <sup>8</sup>Institute of Microbiology, ETH Zürich, Zürich, Switzerland <sup>9</sup>Experimental and Clinical Pharmacology and Toxicology, Saarland University, Homburg, Germany <sup>10</sup>BGI-Shenzhen, Shenzhen 518083, China <sup>11</sup>Department of Medicine, Division of Nephrology, University Medical Center Freiburg, Germany <sup>12</sup>Department of Rheumatology and Clinical Immunology, Medical Center-University of Freiburg, Faculty of Medicine, University of Freiburg, Germany <sup>13</sup>Department of Pediatrics, University Medical Centre Hamburg, Germany <sup>14</sup>Beaumont Child Children's Hospital Troy, Michigan, USA <sup>15</sup>University Hospitals Cleveland Medical Center Allergy-Immunology Fellowship Program Cleveland, Ohio, USA <sup>16</sup>Allergy and Immunology Associates, Inc. Mayfield Hts, Ohio, USA <sup>17</sup>Department of Pediatrics, University of California San Francisco School of Medicine and UCSF Benioff Children's Hospital, San Francisco, California, USA <sup>18</sup>Institute of Immunity and transplantation, UCL, London, United Kingdom

#Address correspondence to: Univ.-Prof. Dr. med. Bodo Grimbacher, Scientific-Director, CCI-Center for Chronic Immunodeficiency, UNIVERSITÄTSKLINIKUM FREIBURG, Tel.: 0761270-77731 Fax: -77744, Breisacherstraße 115, 79106 Freiburg, bodo.grimbacher@uniklinik-freiburg.de, [www.uniklinik-freiburg.de/cci](http://www.uniklinik-freiburg.de/cci).

\*Contact during review: Desirée Schubert; [desiree.schubert@uniklinik-freiburg.de](mailto:desiree.schubert@uniklinik-freiburg.de)

**Publisher's Disclaimer:** This is a PDF file of an unedited manuscript that has been accepted for publication. As a service to our customers we are providing this early version of the manuscript. The manuscript will undergo copyediting, typesetting, and review of the resulting proof before it is published in its final citable form. Please note that during the production process errors may be discovered which could affect the content, and all legal disclaimers that apply to the journal pertain.

### Author contributions

Conceptualization, D.S., B.G., R.Z.; Methodology, D.S., M.F., M.R., H.E.; Software, S.W., S.R., A.B.; Formal Analysis, S.P., A.B.; Investigation, D.S., M.C.K., S.H., L.Y., M.P., Ja.K., Jo.K, S.W., A.A.S., H.C., F.Y., Y.L., J.M.P., A.M., B.P.P.; Resources, H.E., R.K., A.L.M., R.W.H., J.M.P.; Writing – Original Draft, D.S.; Writing – Review & Editing, M.C.K., An.C., A.A.S., J.M.P, R.Z., B.G.; Supervision, D.S., A.A.S., Ad.C., R.Z., B.G.; Funding Acquisition, D.S., B.G., R.Z.

## Abstract

**Background**—Primary antibody deficiencies (PAD) are the most frequent primary immunodeficiencies in humans. The genetic causes for PADs are largely unknown. Sec61 translocon alpha 1 subunit (SEC61A1) is the major subunit of the Sec61 complex, which is the main polypeptide-conducting channel in the endoplasmic reticulum (ER) membrane. *SEC61A1* is a target gene of XBP1s and strongly induced during plasma cell differentiation.

**Objective**—Characterization of a novel genetic defect and its pathological mechanism in eleven patients from two unrelated families with PAD.

**Methods**—Whole exome sequencing (WES) and targeted sequencing were conducted to identify novel genetic mutations. Functional studies were carried out *ex vivo* in primary cells of patients and *in vitro* in different cell lines to assess the effect of *SEC61A1* mutations on B cell differentiation and survival.

**Results**—We investigated two families with patients suffering from hypogammaglobulinemia, severe recurrent respiratory tract infections and normal peripheral B- and T cell subpopulations. Upon *in vitro* stimulation, B cells showed an intrinsic deficiency to develop into plasma cells (PCs). Genetic analysis and targeted sequencing identified novel heterozygous missense (c.254T>A, p.V85D) and nonsense (c.1325G>T, p.E381\*) mutations in *SEC61A1*, segregating with the disease phenotype. SEC61A1-V85D was deficient in co-translational protein translocation and it disturbed the cellular calcium homeostasis in HeLa cells. Moreover, SEC61A1-V85D triggered the terminal unfolded protein response (UPR) in multiple myeloma (MM) cell lines.

**Conclusion**—We describe a monogenic defect leading to a specific plasma cell deficiency in humans, expanding our knowledge about the pathogenesis of antibody deficiencies.

## Keywords

SEC61A1; translocon; protein translocation; antibody deficiency; plasma cell; multiple myeloma; calcium homeostasis; ER stress

## Introduction

Primary antibody deficiencies (PADs) are the most frequent primary immunodeficiencies (PIDs) in humans<sup>1</sup>. PADs are a group of diseases generally characterized by impaired B cell differentiation and function, which results in low immunoglobulin (Ig) production. They have a spectrum of underlying causes and phenotypical expressivity<sup>2</sup>.

Differentiation of B lymphocytes into plasma cells (PCs) requires extensive morphological and homeostatic changes<sup>3</sup> such as the expansion of the endoplasmic reticulum (ER), which allows PCs to become secretory factories releasing thousands of antibodies per second<sup>4</sup>. This massive Ig production is accompanied by the accumulation of misfolded proteins in the ER, which activates the unfolded protein response (UPR). The UPR must be constitutively maintained in plasma cells to cope with perpetual ER stress to ensure longevity<sup>5</sup>. Of the existing signaling pathways regulating the UPR in mammals (IRE1A/XBP1s, PERK/ATF4 and ATF6/ATF6f), only the IRE1A/XBP1s pathway is required for the differentiation of B cells into PCs<sup>6, 7</sup>. After sensing ER stress, inositol-requiring enzyme 1 alpha (IRE1A) is

activated by phosphorylation. Active IRE1A triggers the splicing of the “unspliced” transcriptional activator x-box binding protein 1 (*XBPIu*) by the excision of a 23-base pair intron from its mRNA, resulting in the active “spliced” form of the *XBPI* mRNA (*XBPIs*)<sup>8,9</sup>. *XBPIs* increases the synthetic capacities of cells by inducing the transcription of genes encoding mediators of protein synthesis, transport, folding and degradation<sup>10</sup>. However, which of the many target genes of *XBPIs* are critical for plasma cell differentiation is poorly understood. Interestingly, the PERK/ATF4 pathway of the UPR is specifically suppressed during the differentiation of B cells into PCs<sup>6</sup>. PKR-like ER kinase (PERK) activation leads to a global downregulation of protein synthesis and concomitantly increased levels of the activating transcription factor 4 (ATF4), which induces the transcription of C/EBP homologous protein (*CHOP*). *CHOP* is a mediator of the terminal UPR that induces apoptosis in situations of unresolvable ER stress<sup>11</sup>. Therefore, activation of the PERK/ATF4 pathway would be incompatible with the development of a long-lived humoral immune response.

The genes encoding the Sec61 complex are targets of the UPR<sup>10</sup>. This protein complex co- or post-translationally transports nascent polypeptides from the cytosol into the ER lumen or inserts them into the ER membrane<sup>12</sup>. The heterotrimeric Sec61 complex is composed of the large SEC61A1 subunit and the two much smaller SEC61B and SEC61G subunits<sup>13</sup>. In its open state, the Sec61 channel forms a large aqueous pore in the ER membrane that is penetrable for small molecules and ions<sup>14</sup>. Indeed, the Sec61 complex acts as a passive calcium (Ca<sup>2+</sup>) leakage channel<sup>15</sup>. Therefore, SEC61A1 contains a highly conserved domain called the “pore ring” that tightly surrounds the nascent polypeptide to limit Ca<sup>2+</sup> leakage through the opened channel<sup>13</sup>.

Here, we describe two families suffering from early-onset, severe, recurrent bacterial infections of the respiratory tract with antibody isotype deficiencies involving IgM, IgG and IgA. By whole exome sequencing (WES) in the first family and targeted sequencing in the second family, we identified a heterozygous missense mutation and a heterozygous nonsense mutation in *SEC61A1*. The missense mutation is located within the pore ring of SEC61A1. Affected individuals had normal numbers and subsets of peripheral B cells, but these failed to differentiate into PCs *in vitro*. We show that *SEC61A1-V85D* overexpression boosts ER stress due to an increased Ca<sup>2+</sup> leakage and impaired protein translocation in HeLa cells, and activates the terminal UPR in multiple myeloma (MM) cell lines.

## Materials and methods

### Ethics approval

All individuals donated samples following informed written consent under local ethics board-approved protocols: 295/13\_140782 from 19th August 2014 “Klinik und molekulargenetischer Defekt des variablen Immundefekts (CVID)” (ethics committee of the Albert-Ludwigs-University Freiburg).

## B cell stimulation assay

B cells were isolated from PBMCs with the B cell isolation kit II (Miltenyi Biotec). 30,000 CD19<sup>+</sup> B cells (purity >90%, mostly >99%) were seeded in triplicates for each time point and stimulated in 200 µl medium (IMDM supplemented with 10% FBS, 1% penicillin/streptomycin, 2.5 µg/ml Transferrin, 1 µg/ml Glutathion, 1 µg/ml Insulin, 2 mM L-Glutamine, 1× non-essential amino acids and 0.1% fatty acid supplement) containing 2 µg/ml anti-IgM antibody (SouthernBiotech #2020-10), 0.5 µM CpG (Apara Bioscience #153100) and 0.1 µg/ml Baff-3mer or CD40L and IL21 (Baff-3mer, CD40L and IL21 were produced, titrated and kindly provided by the laboratory of Professor Dr. Eibel) in a 96-well round bottom culture plate for nine days. The medium was changed (100 µl medium were replaced by fresh, twofold concentrated stimulation medium) every three days.

## SEC61A1 silencing and expression

To rescue the phenotype of *SEC61A1* silencing and functionally characterize the SEC61A1-V85D mutant, the respective cDNAs of wild type (wt) or mutant were inserted into the multi-cloning sites of the pCMV6-AC-IRES-GFP-vector (Origene). For gene silencing,  $6 \times 10^5$  HeLa cells were seeded per 6 cm culture plate. The cells were transfected with *SEC61A1*-UTR (CACUGAAAUGUCUACGUUtt) siRNA (Qiagen) or control siRNA (AllStars Negative Control siRNA, Qiagen) using HiPerFect Reagent (Qiagen) for 96 hours as described previously<sup>16</sup> (final concentration of siRNAs: 20 nM). SiRNA transfection was repeated after 24 hours. Six hours after the first siRNA transfection, the cells were transfected with pCMV6 expression plasmids using Fugene HD (Promega).

## Pre-prolactin processing and Cytochrome B5 glycosylation

Two established model precursor polypeptides were used for quantitative analysis of SEC61-dependent (bovine preprolactin (ppl)) as well as SEC61-independent (tail-anchored hybrid protein Cytb5-ops28) protein transport into the ER of semi-permeabilized HeLa cells *in vitro*<sup>17-19</sup>. Both precursor polypeptides were synthesized in reticulocyte lysate (nuclease treated; Promega) in the presence of [<sup>35</sup>S]methionine (Perkin Elmer) plus buffer or semi-permeabilized HeLa cells (final concentration: 40,000 cell equivalents/µl) for 60 minutes at 30°C. Semi-permeabilized-cells were prepared from identical cell numbers by digitonin treatment. Transport of [<sup>35</sup>S]methionine-labeled ppl *via* the Sec61 complex was assessed by SDS-PAGE and phosphorimaging (Typhoon-Trio imaging system, Image Quant TL software 7.0).

## Live cell calcium imaging

HeLa cells were transfected using FuGene HD (Promega) 8h after seeding with *SEC61A1* expression plasmids in combination with a *SEC61B-IRES-SEC61G* encoding pCDNA3-IRES-GFP expression plasmid. Live cell calcium imaging for cytosolic Ca<sup>2+</sup> was carried out as described previously<sup>20</sup>.

## Viral transduction of cell lines

The respective cDNAs of wt or mutant *SEC61A1* were inserted into the multi-cloning sites of the pMXS-IRES-GFP retroviral expression vector. HEK293T cells were transiently

transfected using X-tremeGene HP DNA Transfection Reagent (Roche) with 5 µg expression plasmid and 5 µg pCL-ampho retrovirus packaging vector (Imgenex). The medium was changed after 24 hours and virus was harvested 48 and 72 hours after transfection. Cell lines were treated on two consecutive days with virus-containing medium and fresh medium in a 1:1 ratio. Spin infection was carried out for 2–3 hours at 870 g. Infection efficiencies were analyzed by flow cytometry. Fluorescence activated cell sorting (FACS) was carried out with a MoFlo Astrios cell sorter (Beckman Coulter). Multiple myeloma cells were sorted one day after the second viral transduction. Transduced Hek293T cells were expanded in culture for one week before sorting.

## Results

### Clinical description of the families

We investigated 10 individuals in Family I (Figure 1A), who had antibody isotype deficiencies involving IgM, IgG and IgA (Table S1) and who suffered from severe recurrent bacterial infections such as tonsillitis, otitis, sinusitis, pneumonias and gastrointestinal infections. The disease onset was mostly in the first year of life. Affected individuals did not respond to polysaccharide vaccination and responded variably to *tetanus* toxin vaccination (Table S1). They have successfully maintained a marked decrease in the number and severity of infections since initiating immunoglobulin replacement therapy with intravenous immunoglobulins (IVIG) (detailed case reports in Supplemental Information). The index patient of Family II (Figure 1A) was an eight year old boy who had hypogammaglobulinemia since birth but owing to IVIG treatment has not experienced any severe or recurrent infections (II.P3, detailed case report in Supplemental Information). Attempts to withdraw IVIG treatment repeatedly failed due to persistently low Ig serum levels (Table S1). His mother (who is affected by a secondary immunodeficiency and therefore not included in this study) and grandmother (II.P1) are also mutation carriers; the latter reported an increased frequency of upper respiratory infections during childhood with recurrent bilateral bacterial otitis media. Now, at age 66, she has normal immunoglobulin serum levels (Table S1).

### Identification of heterozygous mutations in *SEC61A1*

We performed linkage analysis using microsatellite markers to identify the genetic region harboring the disease-causing mutation in Family I. A genome-wide scan of all autosomes revealed only one region, on chromosome 3, with LOD scores greater than 2. The high scores were achieved at consecutive markers. Fine mapping confirmed genetic linkage to chromosome 3. The peak single-marker and multiple-marker LOD score was 3.31. The genetic linkage analysis established that the mutated gene should be between markers D3S3697 and D3S3684 (Table S2).

Next, we performed WES on six members of Family I (I.P7, P8, P9, P10, H1 and H2). Evaluation of all variants shared among the four affected individuals and absent in the two unaffected family members revealed three novel single-nucleotide variants (SNV) in the genes *SEC61A1*, *GOLGA8K* and *SLC47A2*, with only *SEC61A1* located in the linkage region on chromosome 3 (Table S3). By Sanger sequencing we confirmed that the

heterozygous missense mutation (c.254T>A, p.V85D) in *SEC61A1* perfectly segregated with the disease within Family I (Figure 1B). c.254T>A in *SEC61A1* translates into a p.Val85Asp change (p.V85D), predicted as “damaging” by programs SIFT<sup>21</sup> (score 0.000), Provean<sup>22</sup> (score -6.26) and MutationTaster<sup>23</sup> (score 4.15). The V85 residue of SEC61A1 (Figure 1C, in magenta) is one of six bulky and hydrophobic amino acids that form the pore ring in the middle of the Sec61 channel (blue and magenta side chains in Figure 1C). Furthermore, V85 is highly conserved (Figure 1D) and a valine to aspartic acid change substitutes a hydrophobic and neutral amino acid for a hydrophilic and negatively charged residue, which is predicted to alter the structure and/or functional properties of the Sec61 channel.

Seeking additional individuals with *SEC61A1* mutations, we performed targeted next generation sequencing in >200 additional patients with primary antibody deficiency. We identified a heterozygous nonsense mutation (c.1325G>T, p.E381\*) in individual II.P3 from Family II (SIFT score: 0.003). By Sanger resequencing, we confirmed this mutation and identified two additional mutation carriers in the family (Figure 1B). In the genome aggregation database (gnomAD) which includes data from 123,136 exomes (ExAc data) and additional 15,496 genomes, there are no mutations reported in healthy individuals leading to a premature stop codon in *SEC61A1*. Moreover, *SEC61A1* was a promising candidate since it is a target gene of XBP1s during plasma cell differentiation<sup>24-26</sup>. As determined by mass spectrometry-based proteomics<sup>27</sup>, the relative abundance of SEC61A protein is two-fold higher in plasmablasts from human peripheral blood as compared to naïve and memory B cells (Figure 1E).

### The p.E381\* nonsense mutation in Family II leads to SEC61A1 haploinsufficiency

Nonsense mutations lead to a premature stop of translation resulting in either the synthesis of a shortened protein or in nonsense-mediated mRNA decay. We analyzed SEC61A1 protein levels in sorted naïve B cells (CD19<sup>+</sup>CD27<sup>-</sup>), and CD3<sup>+</sup>CD4<sup>-</sup> T cells of II.P1 and II.P3. We observed reduced expression levels of SEC61A1 in naïve B cells of II.P1 and II.P3 whereas expression levels in CD8<sup>+</sup> T cells were comparable to the control (Figure 1F). Using a second antibody recognizing the N-terminal domain of SEC61A1 in lysates from an EBV-transformed B cell line of II.P3, we excluded the presence of a shortened protein product from the mutated allele in Family II (Figure S1), supporting the hypothesis that the nonsense mutation p.E381\* likely results in nonsense-mediated mRNA decay and leads to SEC61A1 haploinsufficiency in Family II.

### Affected individuals in both families have normal peripheral B and T cell subpopulations

The circulating B and T cell populations of patients from both families were analyzed by flow cytometry. B-, T- and NK cells were present at normal ratios (Figure 2A and Table S4) and the patients did not show any abnormalities in the detailed T cell phenotyping looking at naïve, memory, and effector T cell stages in CD8<sup>+</sup> and CD4<sup>+</sup> T cells. They also had normal numbers of regulatory T cells and of recent thymic emigrants (Table S4). Even more surprising, the peripheral subpopulations of B cells including naïve, unswitched memory, switched memory, IgA<sup>+</sup>, IgG<sup>+</sup>, transitional and CD21<sup>low</sup> B cells were also normal (Figure 2B, all lymphocyte values are displayed in Table S4). Only the very small population of

peripheral CD27<sup>+</sup>CD38<sup>high</sup> plasmablasts appeared to be reduced in patients of Family I (Figure 2B). However, since this is a very small cell population, which can be lower than 1% of B cells in healthy individuals but increase dramatically during infection, this value is rather error-prone.

### **B cells of mutation carriers have an intrinsic deficiency to develop into plasma cells**

The initial observations on B cells prompted us to study plasma cell development. To assess whether the B cells of patients have an intrinsic differentiation defect, we stimulated purified B cells for nine days mimicking T cell dependent (CD40L and IL21) and T cell independent (anti-IgM, BAFF, CpG) activation. The differentiation of resting peripheral B cells into CD27<sup>+</sup>CD38<sup>high</sup> plasmablasts and CD38<sup>high</sup>CD138<sup>+</sup> plasma cells was significantly decreased in mutation carriers from both families upon T cell dependent (Figure 3A, B) and T cell independent (Figure S2A, B) stimulation. Furthermore, upon CD40L/IL21 stimulation, B cells from affected individuals had decreased IgG and IgA production, but no significantly different IgM production (Figure 3C). Similarly, IgG and IgA levels were significantly lower for cells from affected individuals upon polyclonal stimulation with CpG, BAFF and anti-IgM (Figure S2C), whereas IgM was not secreted by the cells following this stimulation.

### **EBV-transformed B cell lines carrying *SEC61A1* mutations secrete less immunoglobulin**

To substantiate the results of the primary B cell stimulation assay, we studied EBV-transformed B cell lines of several individuals of Family I and II. First, we analyzed protein and mRNA levels in four healthy donor (HD) cell lines, three cell lines generated from Family I and one cell line from II.P3. We observed significantly reduced protein and mRNA levels in all cell lines from patients (Figures 4A and B), with the cell line of II.P3 having the lowest mRNA expression levels (triangle in Figure 4B). If the reduced protein levels were a product of decreased stability of the p.V85D mutant protein, we would have expected similar or even increased mRNA levels in Family I compared to the controls. Since mRNA and protein levels were both reduced and EBV cell lines are known to have a high phenotypic variability, we stained five control and four patient EBV cell lines for B cell surface markers. Intriguingly, we observed that all HD cell lines contained a subpopulation of CD38<sup>high</sup>CD138<sup>+</sup> plasma cells that was absent in all patient-derived cell lines (Figure 4C). This result prompted us to analyze immunoglobulin secretion levels of the cells by ELISPOT. The mean spot size, representing the secretion capacity per cell, was significantly reduced in cells from the patients compared to controls for IgG, IgA and IgM (Figure 4D). Taken together, these data provide a link between low *SEC61A1* expression levels and reduced immunoglobulin secretion by B lymphoblasts.

### **Protein translocation by the *SEC61A1*-V85D channel is impaired**

The main function of *SEC61A1*, as the central subunit of the Sec61 channel, is the transport of nascent polypeptides into the ER. To test whether co-translational protein transport was still functional in mutated translocons, we silenced the endogenous *SEC61A1* mRNA in HeLa cells followed by complementation with either the wt or the mutant *SEC61A1* protein using their respective expression plasmids (Figure 5A). The transport of prolactin (ppl) via the Sec61 complex was assessed in semipermeabilized cells. Ppl is an established model



precursor polypeptide for studying general effects of *SEC61A1* missense mutations on Sec61-dependent cotranslational protein translocation. Upon transport into the ER, the signal peptide of the ppl is cleaved by a signal peptidase leaving the mature prolactin (pl) protein. We observed that co-translational transport of ppl through the SEC61A1-V85D channel was significantly decreased compared to the transport through the wt channel (Figure 5B). In contrast, SEC61A1-independent membrane insertion of the tail-anchored protein Cytochrome B5 and concomitant N-glycosylation was not impaired (Figure 5C), reflecting the integrity of the ER membrane in SEC61A1-V85D-producing cells.

### Dissipation of the ER/cytosol calcium gradient in SEC61A1-V85D-producing HeLa cells

The localization of the p.V85D mutation in the pore ring of SEC61A1 suggested that the ion permeability of the ER membrane, especially concerning the maintenance of the calcium gradient between ER lumen and cytosol, may play a role in the disease pathogenesis. To investigate the influence of the p.V85D mutation on the leakiness of the SEC61A1 channel for Ca<sup>2+</sup> ions, we transiently overproduced SEC61A1-V85D together with its interaction partners SEC61B and SEC61G in HeLa cells (Figure 6A). The cells were then loaded with the calcium indicator Fura2 and treated with thapsigargin, an inhibitor of the SERCA-ATPase, to visualize leakage of calcium from the ER into the cytosol by live cell imaging. Overproduction of the wt protein resulted in an increased leakage (Figure 6B), in accordance with its role as a calcium leak channel. Unexpectedly, we observed a significant decrease in calcium leakage in cells overproducing SEC61A1-V85D compared to cells with endogenous SEC61A1 protein levels or cells overproducing SEC61A1-wt (Figure 6B). This could be explained either by a decreased leakiness of the SEC61A1-V85D channel or, on the contrary, by a severe increase of its leakiness resulting in a depletion of the ER/cytosol Ca<sup>2+</sup> gradient.

Indeed, treating the cells with ionomycin to assess the total amount of calcium ions in the ER lumen revealed that the calcium load of the ER was significantly decreased in cells overproducing the mutant channel in comparison to cells overproducing the wt form (Figure 6C), thus supporting the latter hypothesis. Since these experiments were carried out in cells overexpressing *SEC61A1-V85D* without prior silencing of endogenous *SEC61A1*, we conclude that the effect on the ER/cytosol Ca<sup>2+</sup> gradient is a dominant effect of SEC61A1-V85D.

### SEC61A1-V85D production selectively affects plasma cells

To study the effect of stable expression of *SEC61A1-V85D* on plasma cells, we utilized three different multiple myeloma (MM) cell lines: JK6L, U266 and L-363. While JK6L cells still secrete high amounts of IgG, U266 and L-363 cells do not secrete antibodies (Figure S3); nevertheless, they still have the morphology of plasma cells<sup>28</sup>. Stable transduction with a vector encoding *SEC61A1-V85D-IRES-GFP* resulted in the disappearance of GFP<sup>+</sup> cells of all MM cell lines after several days in culture, whereas the expression of wt *SEC61A1-IRES-GFP* was stable (Figure 7A and S4). Interestingly, the IgG-secreting JK6L cells appeared to be more sensitive to SEC61A1-V85D protein than the non-Ig-secreting U266 and L-363 cells. Stable overexpression of wt and mutant *SEC61A1* in other lymphocytic (EBV-transformed B cells, Jurkat T cells) and non-lymphocytic (THP-1 monocytes,

Hek293T, HeLa, HT29) cell lines did not affect the proliferation capacity or viability of those cells (Figure 7A and S4). Taken together, these observations indicate that SEC61A1-V85D production selectively impairs the survival of plasma cell lines. In line with the hypothesis, patients did not present additional clinical symptoms to infections and lab values of proteins secreted by the liver and the pancreas into the serum were all within the normal ranges (Table S5).

### **SEC61A1-V85D production and SEC61A1 knock down induces the terminal UPR in plasma cell lines**

Based on the experiments in HeLa cells (Figures 5, 6), we hypothesized that disturbed cellular calcium homeostasis and/or dysfunctional protein translocation caused by SEC61A1-V85D might induce unresolvable ER stress and the terminal UPR in MM cells. To study this hypothesis, we analyzed MM cells overproducing SEC61A1-V85D by western blotting (WB) and RT-qPCR. We observed significantly increased protein levels of the ER stress sensors IRE1A and PERK and their downstream transcription factors XBP1s and ATF4 in U266 cells (Figure 7B). Comparable results were obtained from the JK6L (Figure S5A) and the L-363 (Figure S5B) MM cell lines. Notably, the PERK/ATF4 pathway, which acts upstream of the apoptosis-inducing transcription factor CHOP, seemed to be activated. By RT-qPCR analysis, we verified the activation of this pathway. In addition to *XBPIs*, mRNA levels of *ATF4* and *CHOP* were upregulated upon *SEC61A1-V85D* overexpression in L-363 cells (Figure 7C), pointing to the activation of the terminal UPR in this plasma cell line. To study the effect of *SEC61A1* haploinsufficiency on plasma cell homeostasis, we attempted to partially knock down *SEC61A1* in JK6L multiple myeloma cell lines using lentiviral vectors encoding four different shRNAs against *SEC61A1*. However, after puromycin selection, none of the four stably transduced cell lines had reduced SEC61A1 protein levels (data not shown), indicating that we had selected for clones that evaded shRNA knock down while maintaining the puromycin resistance. Next, we directly transfected the cells with siRNA against *SEC61A1*. In independent repeats optimizing the ratio of siRNA to transfection reagent and checking at different time points in JK6L, U266 and L363 cell lines, we found only once a partial knock down of *SEC61A1* at 24 hours post-transfection in JK6L cells. Intriguingly, those cells with a partial knock down had increased expression levels of IRE1A and PERK, showing an increase of ER stress and induction of the UPR (Figure 7E). In summary, these results indicate that multiple myeloma cells do not easily tolerate a knock down of *SEC61A1* and that a knock down might induce the UPR in JK6L cells.

### **Dominant effect of mutant SEC61A1-V85D in sensitized HEK293T cells**

In accordance with the insensitivity of non-MM cell lines to the overexpression of *SEC61A1-V85D* (Figure S4), we did not observe an induction of the terminal UPR in Hek293T nor in HT29 cells (data not shown). This suggested that they were likely able to adapt to the effects of the mutant protein. To sensitize them towards the overproduction of the mutant SEC61A1, we treated HEK293T cells stably overexpressing *SEC61A1-V85D* for 24h with thapsigargin to induce additional ER stress by mimicking a disturbance of the Ca<sup>2+</sup> homeostasis. As expected, we observed a significantly higher induction of *XBPIs* in cells overproducing SEC61A1-V85D compared to cells overproducing the wt protein (Figure

7D). Interestingly, it made no difference whether the mutant was overexpressed alone or co-overexpressed with *SEC61A1-wt* (Figure 7D), thus showing a dominant effect of SEC61A1-V85D.

## Discussion

Currently known genetic causes for antibody deficiencies, some of which are diagnosed as CVID, impair early B-cell development, B cell receptor signaling or the functionality of B- or T-cells in the germinal center reaction<sup>29</sup>. Even though CVID patients suffering only from infections have been reported to present a considerable subset in CVID cohorts (e.g. Resnick et al.: 32% of 473 subjects<sup>30</sup>), hardly any of the known monogenic disorders present with this clinical phenotype<sup>1, 29</sup>. To our knowledge, this is the first monogenic defect that specifically impairs plasma cell homeostasis without interfering with B cell development, activation, and memory formation.

We found two heterozygous *SEC61A1* mutations in patients of two unrelated families with an early-onset, infection-only antibody deficiency and normal (sub-)populations of peripheral B cells. First, a missense mutation in the pore ring affected cotranslational protein transport and increased Ca<sup>2+</sup> leakage from the ER, the latter representing a potential mechanism for a toxic, dominant-negative effect of the mutant over the wt protein. Second, a nonsense mutation abrogated protein production from one of the two *SEC61A1* alleles. It is known that SEC61A1 proteins with severe mutations compete poorly with wt proteins for binding of complex partners and are therefore degraded in a heterozygous situation<sup>31–33</sup>. In plasma cells, concomitant increase of SEC61B and SEC61G levels might stabilize protein levels of previously degraded p.V85D mutants, resulting in the dissipation of the ER/cytosol calcium gradient and increased ER-stress. In addition, plasma cells, in contrast to most other cells, might require two functional *SEC61A1* alleles to sufficiently induce SEC61A1 protein levels for excessive immunoglobulin production. We suggest that *SEC61A1* haploinsufficiency is causing (possibly transient) hypogammaglobulinemia with variable expressivity and incomplete penetrance in Family II. In contrast, a dominant negative mutation in *SEC61A1* resulting in a functional haploinsufficiency in combination with a dominant negative disturbance of the calcium homeostasis may be responsible for the fully penetrant PAD in Family I ranging from transient hypogammaglobulinemia and specific antibody deficiency to CVID.

In humans, Sec61-channelopathies have been linked for example to polycystic liver disease, diabetes, and congenital disorder of glycosylation due to mutations in the translocon-associated proteins SEC63, ERJ6 and SSR4, respectively<sup>34–36</sup>. Moreover, in a mouse model, a homozygous point mutation in *Sec61a1* impaired binding of Sec61a1 to its interaction partner BiP and caused type 1 diabetes<sup>37</sup>. Evidence that variations in the *SEC61* genes may be relevant to plasma cell deficiency comes from a murine study, in which the conditional B cell specific inactivation of *Xbp1* resulted in reduced production of IgM and IgG and in reduced expression levels of the *Xbp1*s target gene *Sec61a1*<sup>25</sup>. A recent study reported two heterozygous missense mutations in *SEC61A1* in patients with autosomal dominant tubulointerstitial and glomerulocystic kidney disease (ADTKD) with anemia<sup>38</sup>. Laboratory values that were found altered in ADTKD patients were normal in our patients (Table S6).

The effects of *SEC61A1* missense mutations in ADTKD on protein-protein interactions, intrinsic functionality, or protein stability were not investigated. However, heterozygous mutations that reduce the hydrophobicity of the signal peptide of renin cause ADTKD with a clinical phenotype similar to the phenotype associated with *SEC61A1* mutations. These mutations interfere with SEC61 complex-dependent translocation of renin across the ER membrane and signal peptide cleavage, hence the Sec61 complex is directly involved in the disease pathogenesis<sup>39–41</sup>. It therefore seems possible that the *SEC61A1* mutations in ADTKD specifically impair renin translocation and processing and therefore mirror the clinical phenotype of renin mutations.

In summary, we provide evidence that the disturbance of the ER homeostasis interferes with plasma cell functionality in humans and can cause primary antibody deficiency as previously proposed by others<sup>42</sup>. We hypothesize that sensors, signaling components and target genes of the UPR that play an important role in protein synthesis, modification and secretion, and in the maintenance of the ER homeostasis in PCs are likely to be mutated or dysregulated in other antibody-deficient patients with normal numbers of peripheral B cells.

## Supplementary Material

Refer to Web version on PubMed Central for supplementary material.

## Acknowledgments

The authors especially thank the patients and their relatives for the participation in this study. We thank Beate Fischer for the production of CD40L and IL21, Kathrin Pieper for the production of BAFF-3mer, Professor Reinhard Voll for kindly providing the JK6L cell line, and Jessica Pfannstiel for the microsatellite genotyping.

This research was funded by the Bundesministerium für Bildung und Forschung (BMBF) with the grant numbers IFB/CCI: 01EO1303; E:med/SysInflame: 012ZX1306F, and DZIF: 8000805-3 (B.G.) and supported in part by the Excellence Initiative of the German Research Foundation (GSC-4, Spemann Graduate School) (D.S.). This work was also supported in part by the Intramural Research Program of the National Institutes of Health, NLM (A.A.S) and by grants from the Deutsche Forschungsgemeinschaft to A.C. (SFB894) and R.Z. (IRTG1830, SFB 894).

## References

1. Picard C, Al-Herz W, Bousfiha A, Casanova JL, Chatila T, Conley ME, et al. Primary Immunodeficiency Diseases: an Update on the Classification from the International Union of Immunological Societies Expert Committee for Primary Immunodeficiency 2015. *J Clin Immunol.* 2015; 35:696–726. [PubMed: 26482257]
2. Fried AJ, Bonilla FA. Pathogenesis, diagnosis, and management of primary antibody deficiencies and infections. *Clin Microbiol Rev.* 2009; 22:396–414. [PubMed: 19597006]
3. Wiest DL, Burkhardt JK, Hester S, Hortsch M, Meyer DI, Argon Y. Membrane biogenesis during B cell differentiation: most endoplasmic reticulum proteins are expressed coordinately. *J Cell Biol.* 1990; 110:1501–11. [PubMed: 2335560]
4. Cenci S, Sitia R. Managing and exploiting stress in the antibody factory. *FEBS Lett.* 2007; 581:3652–7. [PubMed: 17475256]
5. Cox JS, Walter P. A novel mechanism for regulating activity of a transcription factor that controls the unfolded protein response. *Cell.* 1996; 87:391–404. [PubMed: 8898193]
6. Ma Y, Shimizu Y, Mann MJ, Jin Y, Hendershot LM. Plasma cell differentiation initiates a limited ER stress response by specifically suppressing the PERK-dependent branch of the unfolded protein response. *Cell Stress Chaperones.* 2010; 15:281–93. [PubMed: 19898960]

7. Reimold AM, Iwakoshi NN, Manis J, Vallabhajosyula P, Szomolanyi-Tsuda E, Gravalles EM, et al. Plasma cell differentiation requires the transcription factor XBP-1. *Nature*. 2001; 412:300–7. [PubMed: 11460154]
8. Calfon M, Zeng H, Urano F, Till JH, Hubbard SR, Harding HP, et al. IRE1 couples endoplasmic reticulum load to secretory capacity by processing the XBP-1 mRNA. *Nature*. 2002; 415:92–6. [PubMed: 11780124]
9. Yoshida H, Matsui T, Yamamoto A, Okada T, Mori K. XBP1 mRNA is induced by ATF6 and spliced by IRE1 in response to ER stress to produce a highly active transcription factor. *Cell*. 2001; 107:881–91. [PubMed: 11779464]
10. Lee AH, Iwakoshi NN, Glimcher LH. XBP-1 regulates a subset of endoplasmic reticulum resident chaperone genes in the unfolded protein response. *Mol Cell Biol*. 2003; 23:7448–59. [PubMed: 14559994]
11. Li Y, Guo Y, Tang J, Jiang J, Chen Z. New insights into the roles of CHOP-induced apoptosis in ER stress. *Acta Biochim Biophys Sin (Shanghai)*. 2014; 46:629–40. [PubMed: 25016584]
12. Johnson AE, van Waes MA. The translocon: a dynamic gateway at the ER membrane. *Annu Rev Cell Dev Biol*. 1999; 15:799–842. [PubMed: 10611978]
13. Van den Berg B, Clemons WM Jr, Collinson I, Modis Y, Hartmann E, Harrison SC, et al. X-ray structure of a protein-conducting channel. *Nature*. 2004; 427:36–44. [PubMed: 14661030]
14. Park E, Rapoport TA. Preserving the membrane barrier for small molecules during bacterial protein translocation. *Nature*. 2011; 473:239–42. [PubMed: 21562565]
15. Lang S, Schauble N, Cavalie A, Zimmermann R. Live cell calcium imaging combined with siRNA mediated gene silencing identifies Ca(2)(+) leak channels in the ER membrane and their regulatory mechanisms. *J Vis Exp*. 2011:e2730. [PubMed: 21775954]
16. Lang S, Benedix J, Fedeles SV, Schorr S, Schirra C, Schauble N, et al. Different effects of Sec61alpha, Sec62 and Sec63 depletion on transport of polypeptides into the endoplasmic reticulum of mammalian cells. *J Cell Sci*. 2012; 125:1958–69. [PubMed: 22375059]
17. Schlenstedt G, Gudmundsson GH, Boman HG, Zimmermann R. A large presecretory protein translocates both cotranslationally, using signal recognition particle and ribosome, and post-translationally, without these ribonucleoproteins, when synthesized in the presence of mammalian microsomes. *J Biol Chem*. 1990; 265:13960–8. [PubMed: 2380197]
18. Enoch HG, Fleming PJ, Strittmatter P. The binding of cytochrome b5 to phospholipid vesicles and biological membranes. Effect of orientation on intermembrane transfer and digestion by carboxypeptidase Y. *J Biol Chem*. 1979; 254:6483–8. [PubMed: 447730]
19. Jackson RC, Blobel G. Post-translational cleavage of presecretory proteins with an extract of rough microsomes from dog pancreas containing signal peptidase activity. *Proc Natl Acad Sci U S A*. 1977; 74:5598–602. [PubMed: 271987]
20. Lang S, Erdmann F, Jung M, Wagner R, Cavalie A, Zimmermann R. Sec61 complexes form ubiquitous ER Ca<sup>2+</sup> leak channels. *Channels (Austin)*. 2011; 5:228–35. [PubMed: 21406962]
21. Kumar P, Henikoff S, Ng PC. Predicting the effects of coding non-synonymous variants on protein function using the SIFT algorithm. *Nat Protoc*. 2009; 4:1073–81. [PubMed: 19561590]
22. Choi Y, Chan AP. PROVEAN web server: a tool to predict the functional effect of amino acid substitutions and indels. *Bioinformatics*. 2015; 31:2745–7. [PubMed: 25851949]
23. Schwarz JM, Cooper DN, Schuelke M, Seelow D. MutationTaster2: mutation prediction for the deep-sequencing age. *Nat Methods*. 2014; 11:361–2. [PubMed: 24681721]
24. Shaffer AL, Shapiro-Shelef M, Iwakoshi NN, Lee AH, Qian SB, Zhao H, et al. XBP1, downstream of Blimp-1, expands the secretory apparatus and other organelles, and increases protein synthesis in plasma cell differentiation. *Immunity*. 2004; 21:81–93. [PubMed: 15345222]
25. Todd DJ, McHeyzer-Williams LJ, Kowal C, Lee AH, Volpe BT, Diamond B, et al. XBP1 governs late events in plasma cell differentiation and is not required for antigen-specific memory B cell development. *J Exp Med*. 2009; 206:2151–9. [PubMed: 19752183]
26. Shi W, Liao Y, Willis SN, Taubenheim N, Inouye M, Tarlinton DM, et al. Transcriptional profiling of mouse B cell terminal differentiation defines a signature for antibody-secreting plasma cells. *Nat Immunol*. 2015; 16:663–73. [PubMed: 25894659]

27. Rieckmann JC, Geiger R, Hornburg D, Wolf T, Kveler K, Jarrossay D, et al. Social network architecture of human immune cells unveiled by quantitative proteomics. *Nat Immunol.* 2017
28. Nilsson K, Bennich H, Johansson SG, Ponten J. Established immunoglobulin producing myeloma (IgE) and lymphoblastoid (IgG) cell lines from an IgE myeloma patient. *Clin Exp Immunol.* 1970; 7:477–89. [PubMed: 4097745]
29. Bogaert DJ, Dullaers M, Lambrecht BN, Vermaelen KY, De Baere E, Haerynck F. Genes associated with common variable immunodeficiency: one diagnosis to rule them all? *J Med Genet.* 2016; 53:575–90. [PubMed: 27250108]
30. Resnick ES, Moshier EL, Godbold JH, Cunningham-Rundles C. Morbidity and mortality in common variable immune deficiency over 4 decades. *Blood.* 2012; 119:1650–7. [PubMed: 22180439]
31. Junne T, Kocik L, Spiess M. The hydrophobic core of the Sec61 translocon defines the hydrophobicity threshold for membrane integration. *Mol Biol Cell.* 2010; 21:1662–70. [PubMed: 20357000]
32. Taura T, Baba T, Akiyama Y, Ito K. Determinants of the quantity of the stable SecY complex in the *Escherichia coli* cell. *J Bacteriol.* 1993; 175:7771–5. [PubMed: 8253665]
33. Wilkinson BM, Tyson JR, Reid PJ, Stirling CJ. Distinct domains within yeast Sec61p involved in post-translational translocation and protein dislocation. *J Biol Chem.* 2000; 275:521–9. [PubMed: 10617647]
34. Davila S, Furu L, Gharavi AG, Tian X, Onoe T, Qian Q, et al. Mutations in SEC63 cause autosomal dominant polycystic liver disease. *Nat Genet.* 2004; 36:575–7. [PubMed: 15133510]
35. Losfeld ME, Ng BG, Kircher M, Buckingham KJ, Turner EH, Eroshkin A, et al. A new congenital disorder of glycosylation caused by a mutation in SSR4, the signal sequence receptor 4 protein of the TRAP complex. *Hum Mol Genet.* 2014; 23:1602–5. [PubMed: 24218363]
36. Synofzik M, Haack TB, Kopajtich R, Gorza M, Rapaport D, Greiner M, et al. Absence of BiP co-chaperone DNAJC3 causes diabetes mellitus and multisystemic neurodegeneration. *Am J Hum Genet.* 2014; 95:689–97. [PubMed: 25466870]
37. Lloyd DJ, Wheeler MC, Gekakis N. A point mutation in Sec61alpha1 leads to diabetes and hepatosteatosis in mice. *Diabetes.* 2010; 59:460–70. [PubMed: 19934005]
38. Bolar NA, Golzio C, Zivna M, Hayot G, Van Hemelrijk C, Schepers D, et al. Heterozygous Loss-of-Function SEC61A1 Mutations Cause Autosomal-Dominant Tubulo-Interstitial and Glomerulocystic Kidney Disease with Anemia. *Am J Hum Genet.* 2016; 99:174–87. [PubMed: 27392076]
39. Beck BB, Trachtman H, Gitman M, Miller I, Sayer JA, Pannes A, et al. Autosomal dominant mutation in the signal peptide of renin in a kindred with anemia, hyperuricemia, and CKD. *Am J Kidney Dis.* 2011; 58:821–5. [PubMed: 21903317]
40. Bleyer AJ, Zivna M, Hulkova H, Hodanova K, Vyletal P, Sikora J, et al. Clinical and molecular characterization of a family with a dominant renin gene mutation and response to treatment with fludrocortisone. *Clin Nephrol.* 2010; 74:411–22. [PubMed: 21084044]
41. Zivna M, Hulkova H, Matignon M, Hodanova K, Vylet'al P, Kalbacova M, et al. Dominant renin gene mutations associated with early-onset hyperuricemia, anemia, and chronic kidney failure. *Am J Hum Genet.* 2009; 85:204–13. [PubMed: 19664745]
42. Pelletier N, Casamayor-Palleja M, De Luca K, Mondiere P, Saltel F, Jurdic P, et al. The endoplasmic reticulum is a key component of the plasma cell death pathway. *J Immunol.* 2006; 176:1340–7. [PubMed: 16424160]

### Key Messages

*SEC61A1*, a target gene of XBP1s during plasma cell differentiation, was mutated in patients diagnosed with primary antibody deficiency.

The disease phenotype was limited to severe, recurrent infections, mainly of the respiratory tract and patients responded well to immunoglobulin replacement therapy.

All patients had normal subpopulations of B and T cells in the peripheral blood but *in vitro* plasma cell homeostasis was impaired due to unresolvable ER-stress.

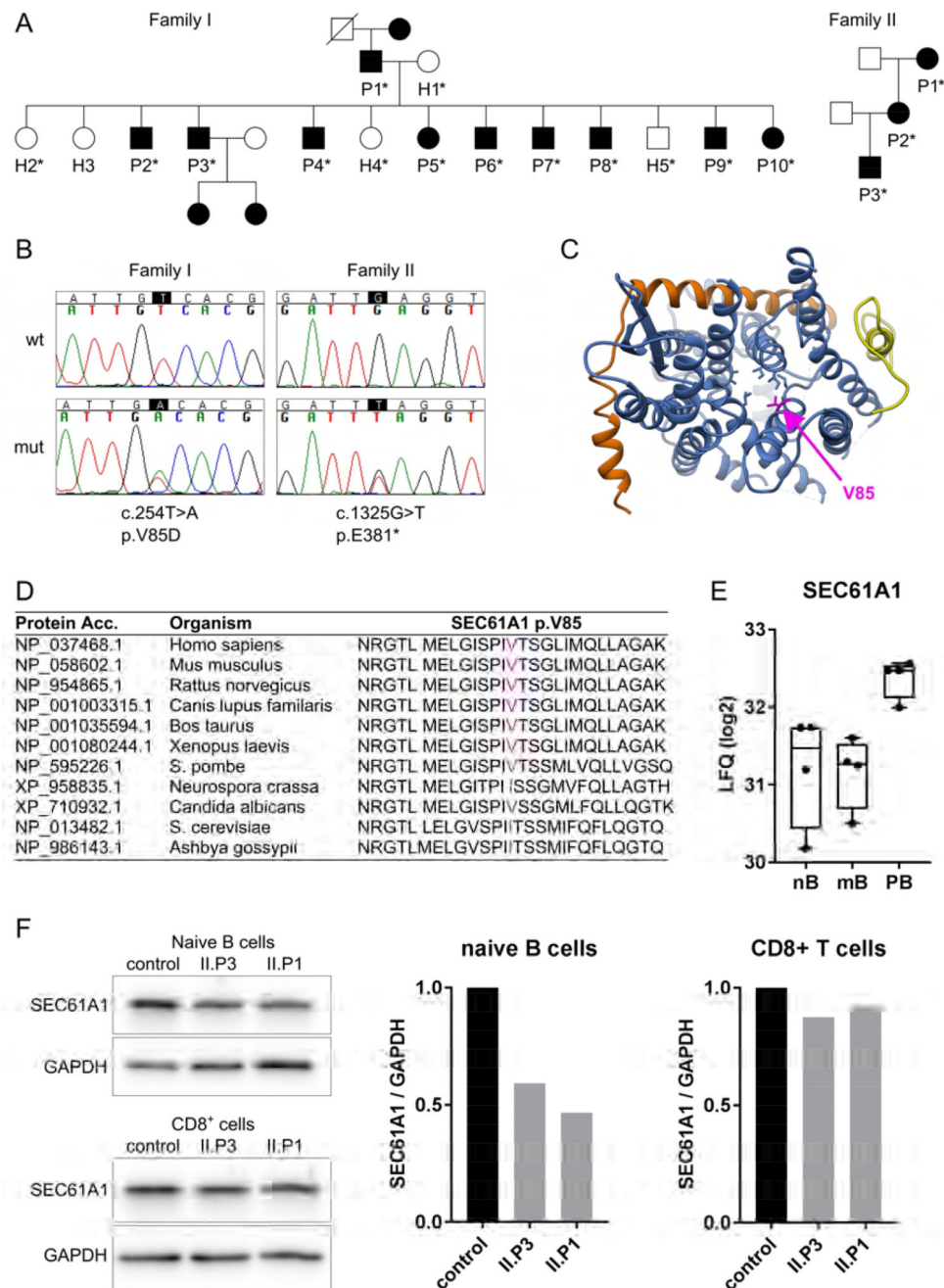


**Figure 1. Mutations in *SEC61A1* in patients with hypogammaglobulinemia**

**A:** Pedigrees of two families with germline *SEC61A1* mutations. Squares: males; circles: females; black filled symbols: mutation carriers; asterisk: genetically tested. **B:** Confirmation of mutations by Sanger sequencing showing the heterozygous changes in the coding sequence (c) and the protein sequence (p). Wt: wild type; mut: mutant. **C:** Atomic model of the heterotrimeric Sec61 complex in the laterally closed conformation seen from the cytoplasm, composed of SEC61A1 (blue), SEC61B (orange) and SEC61G (yellow). Pore ring residues in the center of the channel are shown in blue with the mutated V85 in magenta. The plug domain (transparent) reaches into the pore from the back. **D:** Protein



sequence alignment of SEC61A1 from various species including vertebrates and fungi. The mutated V85 is highlighted in magenta. **E:** Log2 of label free quantitation (LFQ) values of SEC61A1 as determined by mass spectrometry-based proteomics in human cells sorted from peripheral blood. Data were taken from Rieckmann et al.<sup>27</sup>. nB: naïve B cells; mB: memory B cells; PB: plasmablasts **F:** Western blot analysis of SEC61A1 levels in sorted primary CD19<sup>+</sup>CD27<sup>-</sup> naïve B cells and CD3<sup>+</sup>CD4<sup>-</sup> T cells. Bar graphs show the quantification of the blots with SEC61A1 normalized to GAPDH levels.

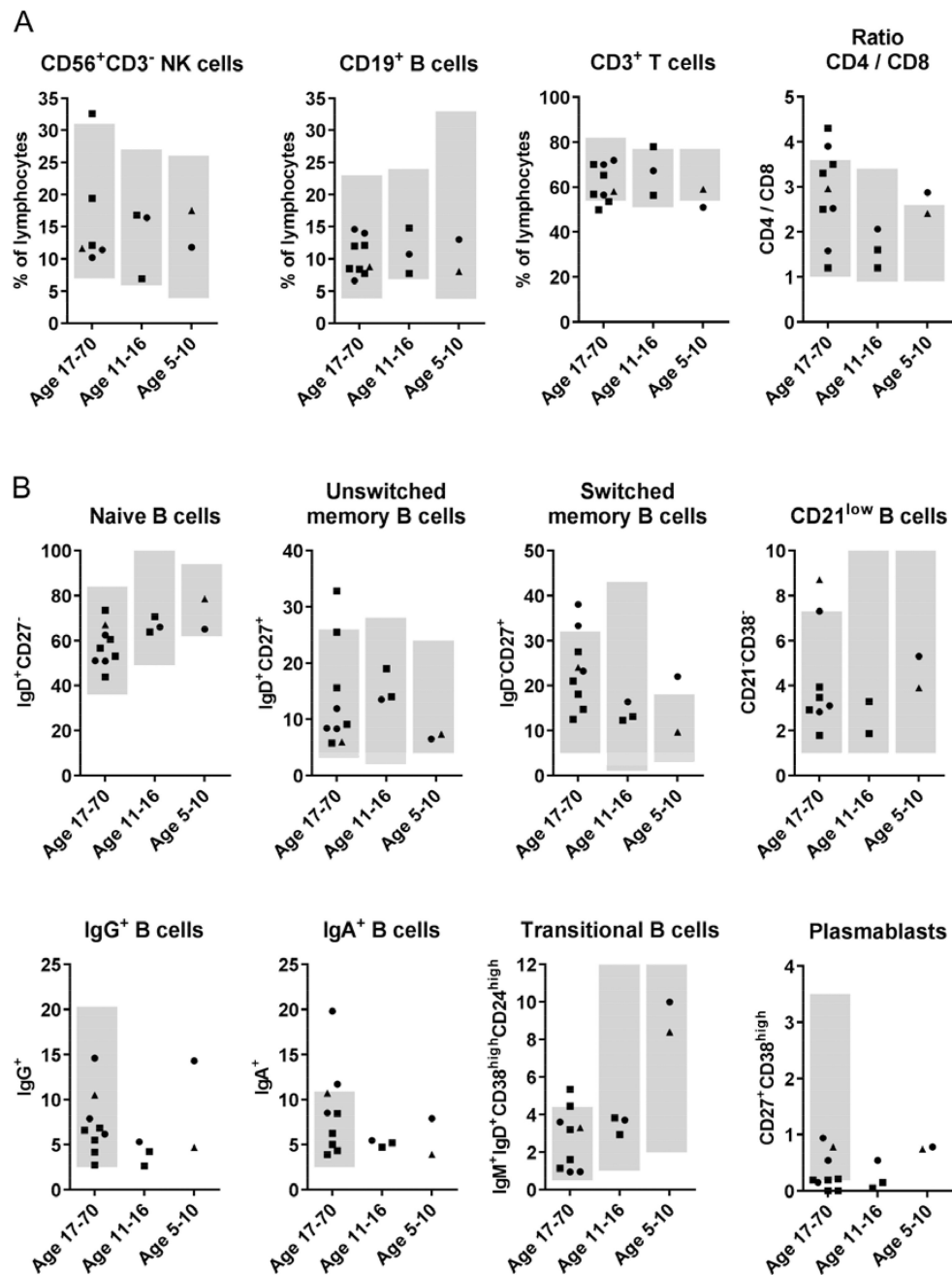


**Figure 2. Flow cytometric analysis of PBMCs**

Relative amount of indicated cells among peripheral blood lymphocytes (**A**) or among CD19<sup>+</sup> B cells (**B**) of patients from Family I (squares), Family II (triangles) and travel controls (circles) divided in three age groups. Grey background indicates the normal range for each age group.

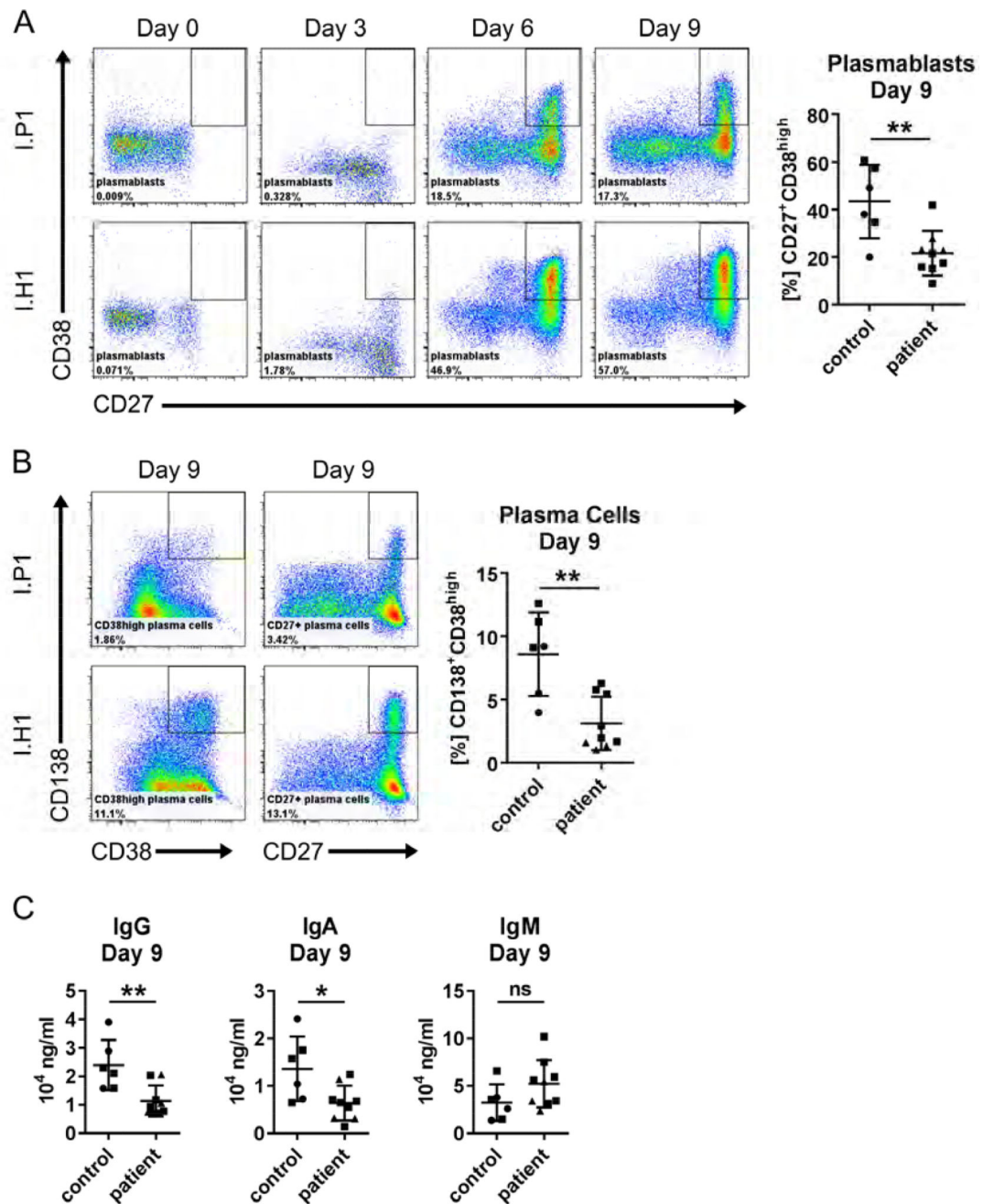


**Figure 3.** *In vitro* differentiation of primary B cells into plasma cells upon stimulation with CD40L and IL21

Scatter plots summarize results of independent experiments for travel controls (circles) and patients of Family I (squares) and Family II (triangles). **A:** Representative flow cytometry plots showing CD38<sup>high</sup>CD27<sup>+</sup> plasmablasts among CD19<sup>+</sup> primary B cells. **B:** Representative flow cytometry plots showing CD38<sup>high</sup>CD138<sup>+</sup> and CD27<sup>+</sup>CD138<sup>+</sup> plasma cells among CD19<sup>+</sup> primary B cells. **C:** Ig in the cell culture supernatant measured by ELISA upon CD40L/IL21 stimulation at Day 9. Data are represented as mean  $\pm$  SD; \*\* $p < 0.005$ , \* $p < 0.05$ , ns: not significant (unpaired t test).

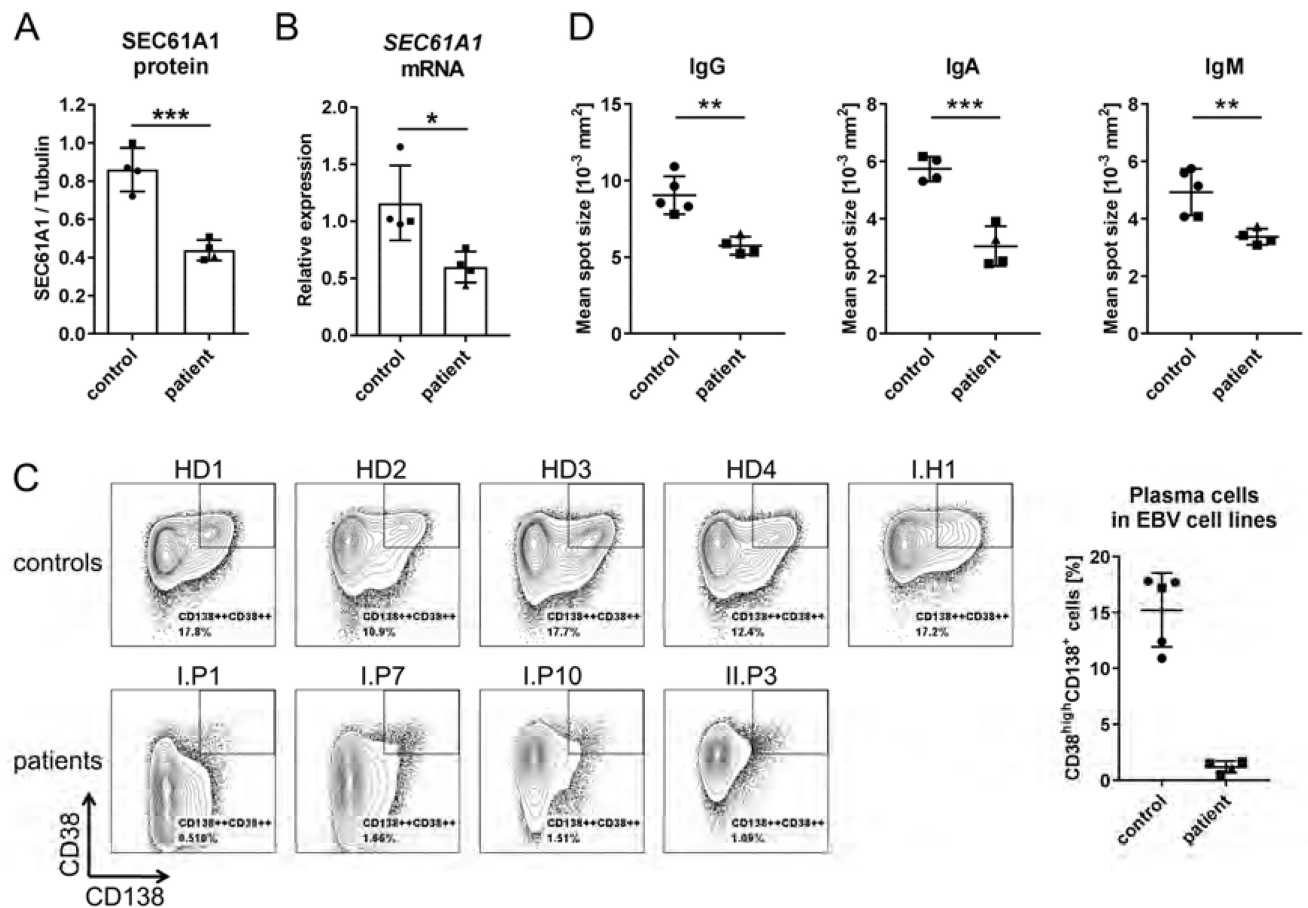


**Figure 4. Analysis of the phenotype of EBV-transformed B cell lines SEC61A1 mutation carriers**  
 Data are shown for subjects of Family I (squares), Family II (triangles) and unrelated healthy donors (HD) (circles). **A:** Quantification of Western blot analysis of SEC61A1 relative to tubulin levels in four HD EBV cell lines and four cell lines from different patients. (n=2) **B:** SEC61A1 mRNA levels relative to the reference genes *HPRT*, *TBP*, *RPLP0* in EBV cell lines from (A). (n=1) **C:** Flow cytometric analysis of surface marker expression in five HD and four patient EBV cell lines. The bar graph indicates the frequency of CD38<sup>high</sup>CD138<sup>+</sup> cells per cell line. **D:** ELISPOT analysis of the mean spot size of secreted IgG, IgA and IgM. Data in bar graphs are represented as mean  $\pm$  SD, ns: not significant, \*p<0.05, \*\*p<0.005, \*\*\*p<0.001 (unpaired t test).

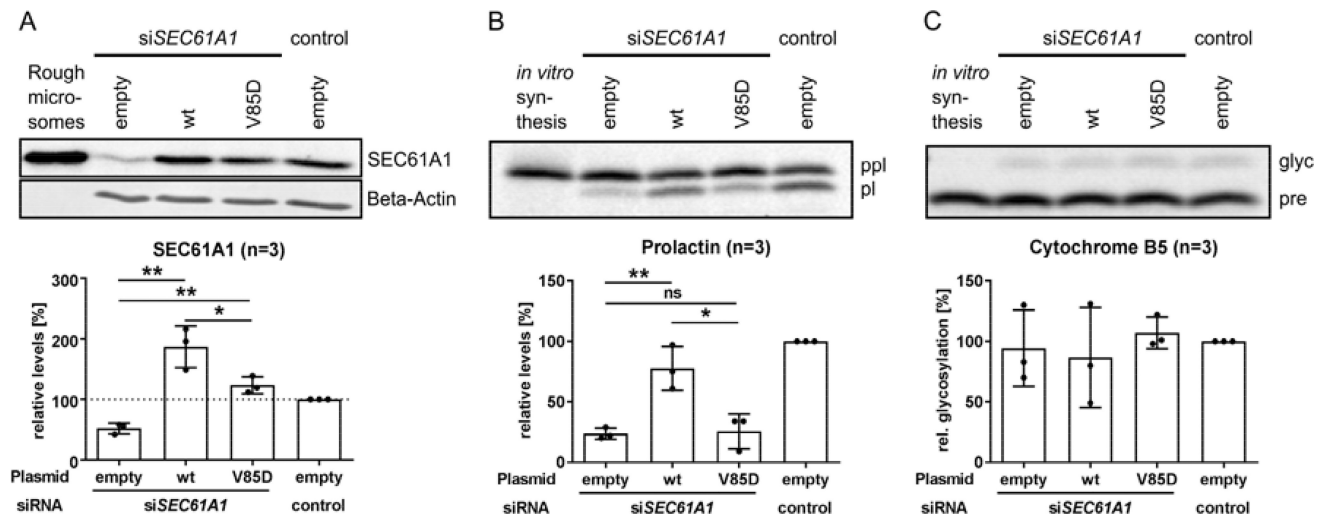


**Figure 5. Effect of p.V85D on Sec61 complex-dependent co-translational protein translocation into the ER**

**A:** Representative Western blot and respective quantification of SEC61A1 levels in HeLa cells treated with the indicated siRNA and transiently transfected with the indicated plasmids. **B:** Representative phosphorimaging blot and respective quantification of the efficiency of co-translational transport of pre-prolactin (ppl) into the ER by HeLa cells given as relative percentage of mature, processed protein prolactin (pl). **C:** Representative phosphorimaging blot (n=3) of the efficiency of Sec61 complex-independent post-translational transport of pre-Cytochrome B5 (pre) into the ER (in HeLa cells) given as the relative percentage of mature, glycosylated protein (glyc). Data are represented as mean  $\pm$  SD; ns: not significant, \* $p < 0.05$ , \*\* $p < 0.005$  (unpaired t test).

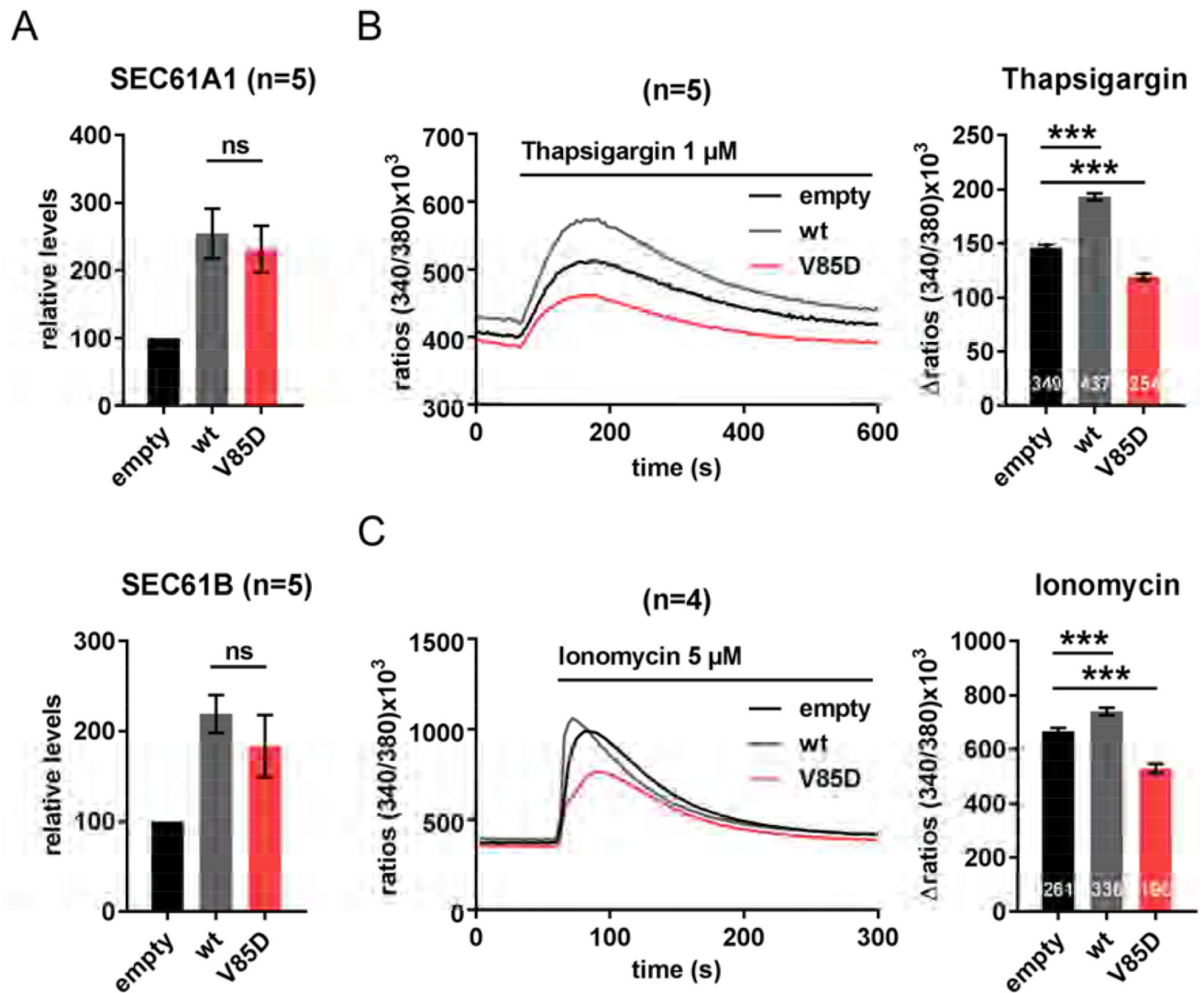


**Figure 6. Effect of SEC61A1-V85D on Ca<sup>2+</sup> leakage from the ER into the cytosol**

**A:** Protein levels of SEC61A1 and SEC61B two days after transient transfection of HeLa cells relative to endogenous levels. Data (n=5) represented as mean  $\pm$  SEM, ns: not significant (unpaired t-test). **B:** Thapsigargin-treatment and live cell imaging of calcium-indicator (Fura-2) loaded in HeLa cells overproducing SEC61A1 (n=5). **C:** Ionomycin-treatment and live cell imaging of calcium-indicator (Fura-2) loaded in HeLa cells overproducing SEC61A1 (n=4). **B** and **C:** Data in bar graphs represented as mean  $\pm$  SEM with the total number of analyzed cells shown at the bottom of the bars. \*\*\*p<0.001 (unpaired t test).

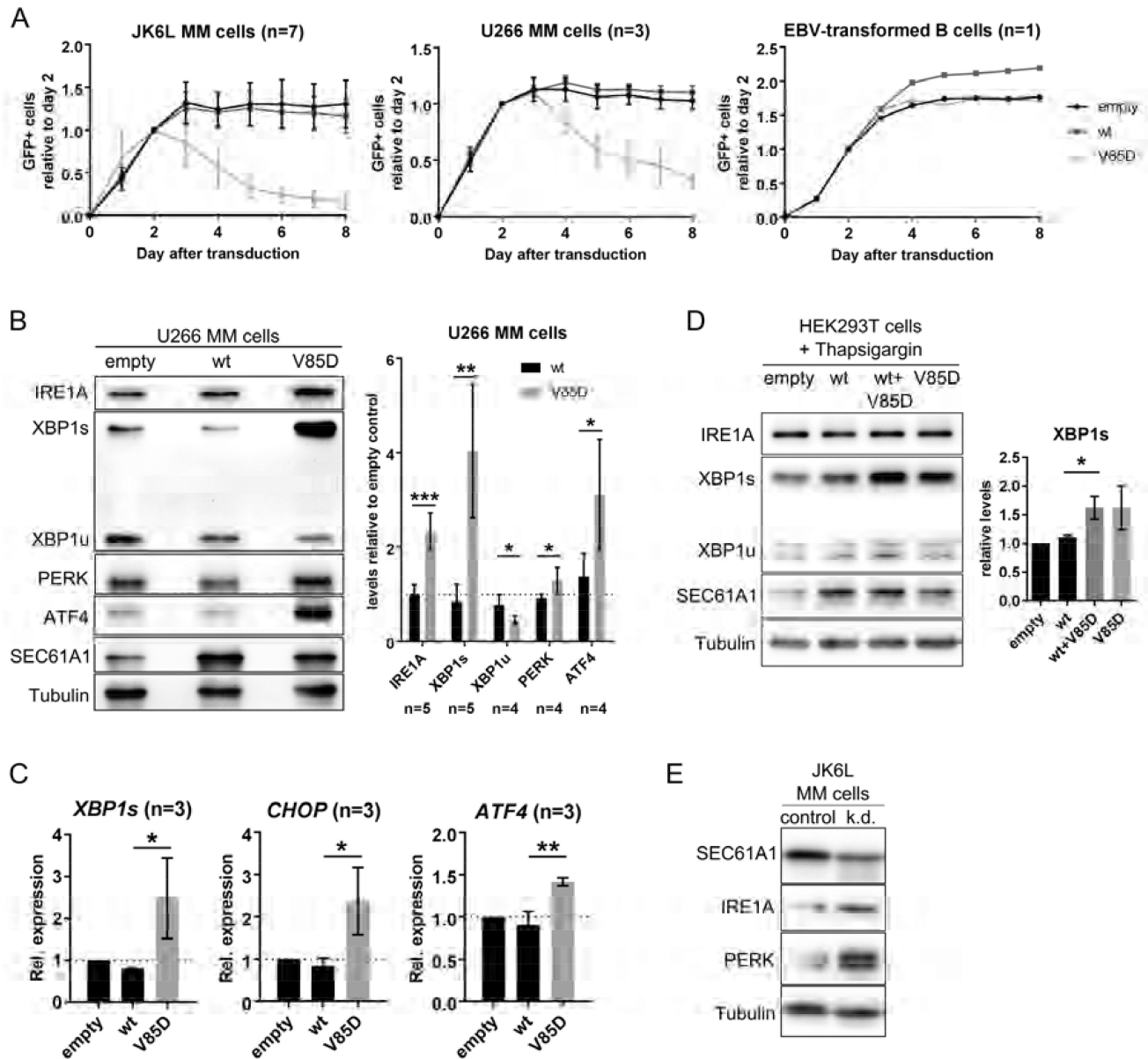


**Figure 7. Effect of UPR induction on plasma cells and sensitized Hek293T cells after SEC61A1-V85D overproduction**

**A:** Flow cytometric analysis of the indicated cell lines after stable transduction with an expression vector encoding SEC61A1-wt or -V85D and GFP separated by an IRES site. **B:** Representative Western blots and respective statistical analysis showing levels of the indicated proteins in U266 cells stably overexpressing *SEC61A1-wt* and -V85D normalized to tubulin levels and relative to cells transduced with the empty vector. **C:** Relative mRNA expression of the indicated transcription factors in L363 cells stably overexpressing *SEC61A1-wt* or -V85D. **D:** Representative Western blots showing levels of the indicated proteins in Thapsigargin-treated Hek293T cells stably overexpressing *SEC61A1-wt* and/or -V85D (n=4). The bar graph shows the respective statistical analysis of XBP1s levels normalized to tubulin levels and relative to cells transduced with the empty vector. **E:**

Western blot (n=1) showing levels of indicated proteins in JK6L cells treated for 24 hours with siRNA against *SEC61A1*. Data in bar graphs is represented as mean  $\pm$  SD, ns: not significant, \*p<0.05, \*\*p<0.005, \*\*\*p<0.001 (unpaired t test).

Author Manuscript

Author Manuscript

Author Manuscript

Author Manuscript